

Biaxial Strain-modified Acceptor Activation Energy of Wurtzite GaN

Analyzed by k·p Method

Lili Ji, Ning Su, John Simon

Department of Electrical Engineering, University of Notre Dame, Notre Dame, IN 46556, USA

The acceptor activation energy change with biaxial strain in wurtzite Gallium Nitride is calculated based on the analysis of strain induced band structure modification. We found a small tensile strain 0.107% in the c-plane separated the heavy hole and light hole bands and makes the light hole band jump above the heavy hole band. This effect results in a reduction in the acceptor activation energy and an increase of hole concentration. The quantitative values of effective mass, mobility and conductivity with different strain are also presented in this work. This theoretical analysis shows a potential way to improve the p-GaN electrical properties by introducing biaxial strains.

I. Introduction

Gallium nitride (GaN) and related nitride materials have received extensive attention due to the device applications such as blue LEDs, blue lasers, and high power electronic devices. A great deal of effort has been devoted to growing sufficiently high quality GaN thin films for these applications. III-V Nitride semiconductors crystallize in the wurtzite structure when grown on most common substrates such as (0001)-oriented sapphire or SiC. The lattice mismatch between bulk GaN and sapphire or SiC gives rise to a large biaxial strain in the GaN epilayer of -13% and 4%, respectively [1]. Additional biaxial

strain originates from the post growth cooling [2]. To better understand the electrical properties of III-V Nitride semiconductors and devices with biaxial strain, fundamental studies of the wurtzite band structure is of great importance. Although the strain influence on GaN bandstructure has been studied and presented using the k-p method [3], to our best knowledge, little work has been done to apply the results to investigate the biaxial strain-modified acceptor activation energy in wurtzite GaN. That serves the motivation for this work.

The activation of p-type dopant in GaN material has long been an important issue for the production of III-V Nitride based devices. Magnesium is the most commonly used acceptor dopant in III-V Nitride semiconductors and the thermal activation energy is reported between 120meV and 250meV using various characterization techniques such as Hall-effect, thermal admittance spectroscopy (TAS), and current deep-level transient spectroscopy (I-DLTS) measurements [4]. Because of the deep nature of the Mg dopant, very high doping level (approximately 10^{20} cm^{-3}) has to be used for device structure to get the hole concentration in the order of 10^{18} cm^{-3} . [5]

In this paper, the effect of the biaxial strain on the Mg-activation energy has been analyzed. The calculation is valid under the assumption that the Mg dopant energy level is fixed relative to the vacuum level in the band structure under various strains. In this case, the change of acceptor activation energy induced by strain is a direct result of the band structure modification. Applying the k-p perturbation method, the conduction and valence bands dispersion near the band edge have been calculated under both

compressive and tensile strains. Our work also presents a more accurate result for band structure calculation under strain because we use the completely up-to-date band structure parameters given by Vurgaftman and Meyer[6], some of which are quite different from the values used in earlier papers, for example, the deformation potentials. This work helps to clarify some inconsistencies in the choices of band structure parameters and gives updated results to researchers in this field.

II. Effective-mass Hamiltonian for conduction and valence bands under strain

Considering a strained layer with wurtzite crystal structure pseudomorphically grown along (0001) direction (z-axis), the strain tensor has the only nonvanishing elements as

$$\varepsilon_{xx} = \varepsilon_{yy} = \frac{a_0 - a}{a}; \quad \varepsilon_{zz} = -\frac{2C_{13}}{C_{33}}\varepsilon_{xx} \quad (1)$$

Where a and a_0 are the lattice constants for the epilayer and substrate. C_{13} and C_{33} are the stiffness coefficients.

The bulk valence-band structure can be determined by finding the eigenvalues of the Hamiltonian:

$$\det[H_{6 \times 6}^v(k) - I_{6 \times 6} E^v(k)] = 0 \quad (2)$$

where k is the wave vector and $I_{6 \times 6}$ is the unit matrix.

The 6x6 Hamiltonian for the valence-band structure has been derived by the k·p method taking account the strain effect [3]. It can be block diagonalized using a unitary transformation [7]

$$H_{6 \times 6}^v(k) = \begin{bmatrix} H_{3 \times 3}^U(k) & 0 \\ 0 & H_{3 \times 3}^L(k) \end{bmatrix} \quad (3)$$

$$H_{3 \times 3}^U(k) = \begin{bmatrix} F & K_t & -iH_t \\ K_t & G & \Delta - iH_t \\ iH_t & \Delta + iH_t & \lambda \end{bmatrix} \quad (4)$$

$$H_{3 \times 3}^L(k) = \begin{bmatrix} F & K_t & iH_t \\ K_t & G & \Delta + iH_t \\ -iH_t & \Delta - iH_t & \lambda \end{bmatrix} \quad (5)$$

where

$$\begin{aligned} F &= \Delta_1 + \Delta_2 + \lambda + \theta \\ G &= \Delta_1 - \Delta_2 + \lambda - \theta \\ \lambda &= \frac{\hbar}{2m_0} (A_1 k_z^2 + A_2 k_t^2) + D_1 \epsilon_{zz} + D_2 (\epsilon_{xx} + \epsilon_{yy}), \\ \theta &= \frac{\hbar}{2m_0} (A_3 k_z^2 + A_4 k_t^2) + D_3 \epsilon_{zz} + D_4 (\epsilon_{xx} + \epsilon_{yy}), \\ K &= \frac{\hbar}{2m_0} A_5 k_t^2, \\ H_t &= \frac{\hbar}{2m_0} A_6 k_t k_z, \\ \Delta &= \sqrt{2} \Delta_3, \end{aligned} \quad (6)$$

and $k_t = \sqrt{k_x^2 + k_y^2}$ is the magnitude of the wave factor in the k_x - k_y plane, A_i s correspond to the Luttinger parameters γ_i s in zinc-blend crystals, Δ_1 is the crystal-field split energy caused by the anisotropy of the wurtzite symmetry, Δ_2 and Δ_3 account for spin-orbit interactions in wurtzite crystals[5], and the D_i s are the Bir-Pikus deformation potentials. The Hamiltonian given in Eqn. (3) has the basis defined as [3]

$$\begin{aligned}
|1\rangle &= \alpha^* |u_1\rangle + \alpha |u_5\rangle \\
|2\rangle &= \beta |u_1\rangle + \beta^* |u_4\rangle \\
|3\rangle &= \beta^* |u_3\rangle + \beta |u_6\rangle \\
|4\rangle &= \alpha^* |u_1\rangle - \alpha |u_5\rangle \\
|5\rangle &= \beta |u_2\rangle - \beta^* |u_4\rangle \\
|6\rangle &= -\beta^* |u_3\rangle + \beta |u_6\rangle
\end{aligned} \tag{7}$$

where

$$\begin{aligned}
u_1 &= \left| -\frac{(X+iY)}{\sqrt{2}} \uparrow \right\rangle, & u_2 &= \left| \frac{(X-iY)}{\sqrt{2}} \uparrow \right\rangle, & u_3 &= |Z \uparrow\rangle; \\
u_4 &= \left| \frac{(X-iY)}{\sqrt{2}} \downarrow \right\rangle, & u_5 &= \left| -\frac{(X+iY)}{\sqrt{2}} \downarrow \right\rangle, & u_6 &= |Z \downarrow\rangle.
\end{aligned} \tag{8}$$

$$\alpha = \frac{1}{\sqrt{2}} e^{i(\frac{3\pi}{4} + \frac{3\phi}{2})}, \quad \beta = \frac{1}{\sqrt{2}} e^{i(\frac{\pi}{4} + \frac{\phi}{2})}$$

Here, $\phi = \tan^{-1}(k_x / k_y)$ is in the k_x - k_y plane and it covers a range between 0 and 2π .

$|X\rangle, |Y\rangle, |Z\rangle$ are defined as p-like wave functions having their dipoles along the $[11\bar{2}0]$, $[\bar{1}\bar{1}00]$ and $[0001]$ direction, respectively [12]. Without considering the spin-orbit coupling effect, the X, Y, Z states are given by

$$\langle X | H_0 | X \rangle = \langle Y | H_0 | Y \rangle = E_v + \Delta_1 + \theta_\varepsilon + \lambda_\varepsilon, \quad \langle Z | H_0 | Z \rangle = E_v + \lambda_s, \tag{9}$$

where E_v is the reference energy.

For non-vanishing Δ_2 and Δ_3 , the general formulas for energy splitting including the strain effect are given by

$$\begin{aligned}
E_c &= E_g + \Delta_1 + \Delta_2 + P_{ce}, \\
E_1 &= \Delta_1 + \Delta_2 + \theta_\varepsilon + \lambda_\varepsilon, \\
E_2 &= \frac{\Delta_1 - \Delta_2 + \theta_\varepsilon}{2} + \lambda_\varepsilon + \sqrt{\left(\frac{\Delta_1 - \Delta_2 + \theta_\varepsilon}{2}\right)^2 + 2\Delta_3^2}, \\
E_3 &= \frac{\Delta_1 - \Delta_2 + \theta_\varepsilon}{2} + \lambda_\varepsilon - \sqrt{\left(\frac{\Delta_1 - \Delta_2 + \theta_\varepsilon}{2}\right)^2 + 2\Delta_3^2},
\end{aligned} \tag{10}$$

Where $P_{c\varepsilon}$ is the hydrostatic energy shift in the conduction band defined as

$$P_{c\varepsilon} = a_{cz}\varepsilon_{zz} + a_{ct}(\varepsilon_{xx} + \varepsilon_{yy}) \quad (11)$$

a_{cz} and a_{ct} are the conduction-band deformation potentials along the x axis and perpendicular to the c axis respectively.

Figure 1 shows the band edge energies with spin-orbit effect included, where the reference energy E_3 has been set to be zero without spin-orbit interaction. In general, if $\Delta_1 > \Delta_2 > 0$, the three bands from top to bottom can be labeled as heavy-hole (HH), light-hole (LH) and crystal-field split-off hole (SO) respectively. Under cubic approximation [8], $\Delta_2 = \Delta_3 = 1/3 \Delta_{so}$, Δ_{so} is the spin-orbit split-off energy.

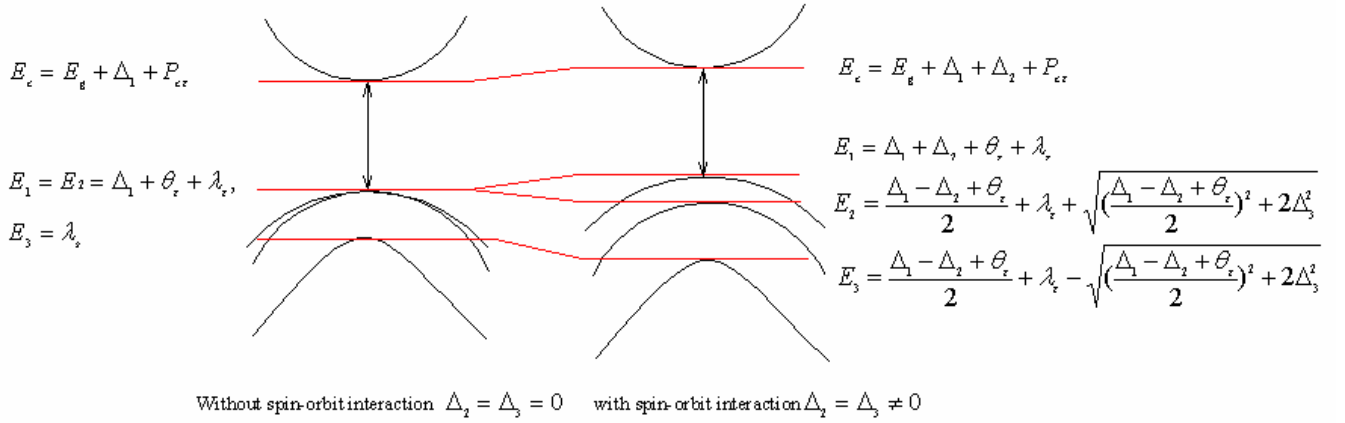


Figure 1: Schematic diagram for band structures with and without spin-orbit interactions.

Knowing the band structure parameters such as A_1s , Δ_1 , Δ_2 and the deformation potentials, the valence band structures can be calculated by finding the eigenvalues of the Hamiltonian given in Eqn. (4).

The conduction band calculation is treated separately here. Applying the parabolic-band model, the effective-mass Hamiltonian can be written as [9]

$$H^c(k_t, k_z) = \left(\frac{\hbar^2}{2}\right)\left(\frac{k_t^2}{m_e^t} + \frac{k_z^2}{m_e^z}\right) + E_c \quad (12)$$

where E_c is given in Eqn. (10), m_e^t and m_e^z are the electron effective masses perpendicular and parallel to the c direction respectively.

III. Calculated band structures and acceptor activation energy change under tensile and compressive strain

With the effective-mass Hamiltonian (including the effect of strain) shown in Section II, the band structure of GaN can be obtained by finding the eigenvalues of the Hamiltonians. Table 1 lists all the band structure parameters used in this calculation.

In Fig. 2, we present the calculated energy values at the band edge of conduction band, heavy hole (HH) band, light hole (LH) band and crystal-field split-off hole (SO) band as a function of strain as well as the equivalent change in band gap for wurtzite GaN. We use the convention ϵ_{xx} to be positive for tensile and negative for compressive strain. With increasing compressive strain, the band gap increases. Under the effect of tensile strain, the light hole (LH) band is pushed upwards, which will lower the band gap at a faster rate. At the tensile strain of 0.107%, the LH band edge rises above the HH band edge.

Fig. 3 shows the valence band structure of GaN under various strains as a function of k_x and k_z , which are transverse and longitudinal axes along [0001] direction.

Table 1 band structure parameters used in the calculation. All the parameters are taken from Reference [3]

Parameters	GaN
Lattice constants (\AA) ^a	
A	3.189
C	5.185
Energy parameters(eV)	
Eg at 300 K	3.510
$\Delta_1=\Delta_{cr}$	0.01
Δ_{so}	0.017
$\Delta_1=\Delta_2=\Delta_{so}/3$	0.0057
Conduction band effective masses ^a	
m_{ez}/m_0	0.2
m_{et}/m_0	0.2
Valence band effective-mass ^a	
A1	-7.21
A2	-0.44
A3	6.68
A4	-3.46
A5	-3.40
A6	-4.9
Deformation potentials (eV) ^a	
$a_{cz}=a_{ct}$	-4.08
D ₁	-3.7
D ₂	4.5
D ₃	8.2
D ₄	-4.1
Elastic stiffness constants (dyn/cm ²) ^a	
C ₁₃	$1.6 \cdot 10^{12}$
C ₃₃	$3.98 \cdot 10^{12}$

^areference [3] 10^{12}

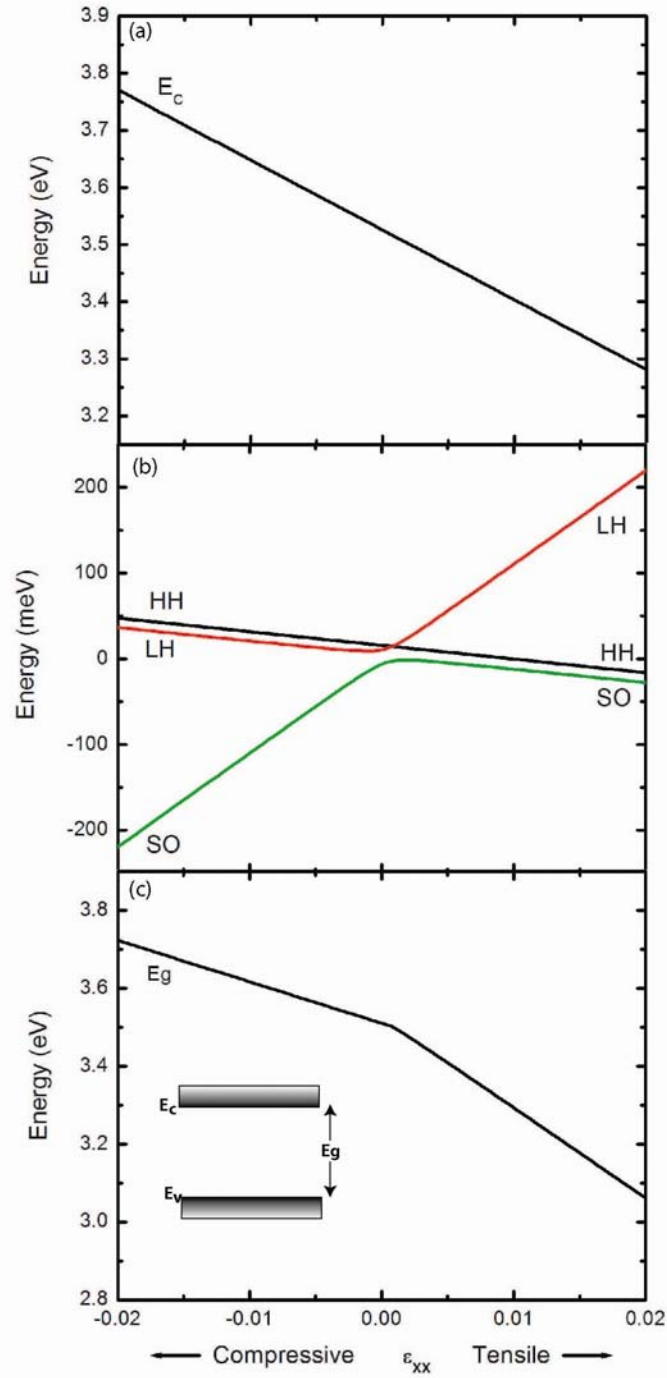


Figure 2: energy values for conduction band (a), HH, LH, SO at the band edge (b) and Band gap (c) as a function of tensile and compressive strain up to 2.0%. The reference energy in equation (9) is set to 0 at the SO band edge with no strain.

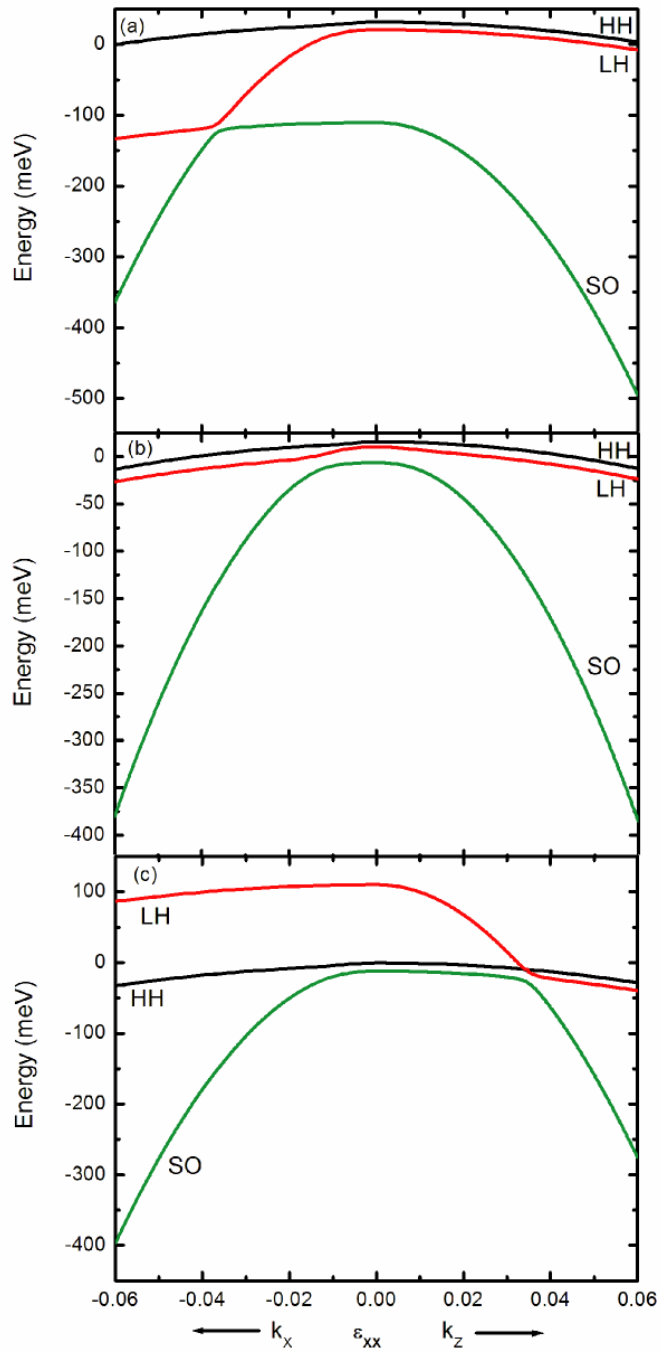


Figure 3: valence band dispersions for (a) 1% compressively strained, (b) unstrained case, and (c) 1% tensile strained GaN wurtzite crystal.

The acceptor activation energy (E_A) for Mg-doped GaN as a function of strain is shown in Figure 4. We assume that E_A doesn't change with respect to vacuum level, and the value of 160meV is used for E_A without strain [10]. The result shows that the activation energy will decrease with either tensile or compressive strain, but a stronger effect is seen under tensile strain.

Applying tensile strain appears to be the most effective way to reduce the Mg activation energy as 1% tensile strain reduces E_A by 50%. As mentioned above, this calculation is valid assuming the Mg dopant level is fixed with respect to the vacuum level under various strain conditions. A direct result from the reduction in acceptor activation energy is that the hole concentration might increase in the bulk GaN material.

We also calculated the density of states g_v for heavy hole, light hole and split off hole by counting the allowed (k_x, k_y, k_z) combinations that will give the electron an energy between E and $E+dE$.

Hole concentration thus can be calculated numerically by the following equations [13]

$$p = \int_{E_{bottom}}^{E_v} g_v (E)[1 - f(E)]dE$$

$$p \approx N_A^- \tag{13}$$

$$\frac{N_A^-}{N_A} = \frac{1}{1 + g_A e^{(E_A - E_F) / kT}}$$

Where g_A is the valence band degeneracy factor (2 for GaN). A Mg doping (N_A) of 10^{18}cm^{-3} was assumed. The sum of hole concentration including HH,LH,SO is presented in Figure 5 as a function of strain. A Mg doping (N_A) of 10^{18}cm^{-3} was assumed and the

compensating defects (N_D) are assumed to be negligible in our example. The tensile strain induced in the bulk crystal appears to greatly increase the hole concentration.

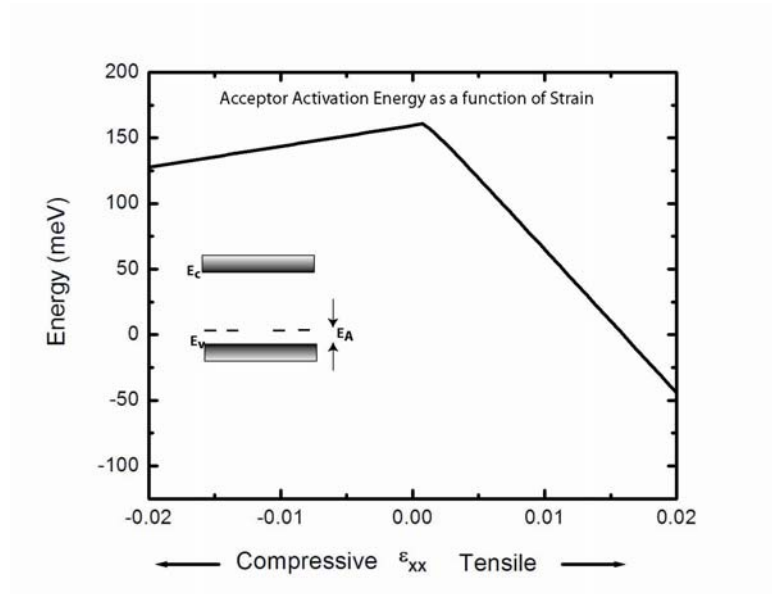


Figure 4: Acceptor activation energy in Mg-doped GaN material under -2% compressive strain to 2% tensile strain. $E_a=160\text{meV}$ is chosen for GaN bulk material without strain.

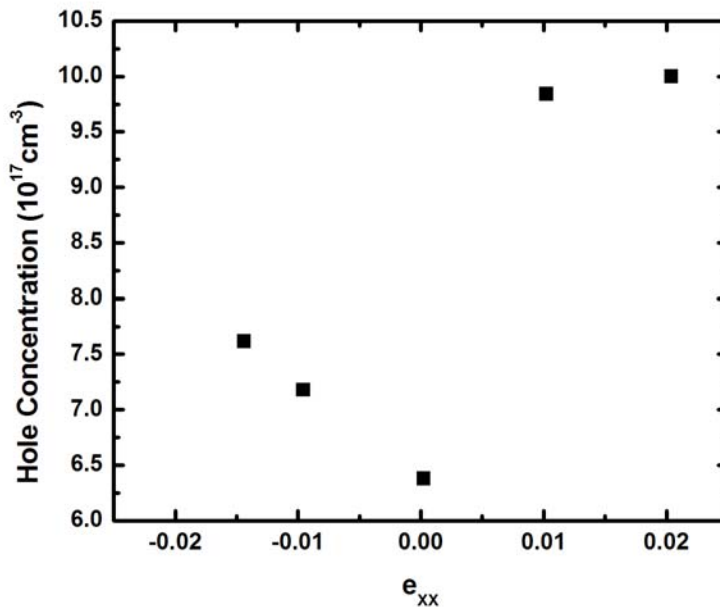


Figure 5: Hole concentration as a function of strain

From the calculated band structure, we can get the effective mass for heavy hole, light hole, split-off hole respectively [3]

$$\begin{aligned}
 m_{hhz} / m_0 &= -1 / (A_1 + A_3) \\
 m_{hht} / m_0 &= -1 / (A_2 + A_4) \\
 m_{lhz} / m_0 &= -1 / (A_1 + \frac{E_{lh0} - \lambda_\epsilon}{E_{lh0} - E_{so0}} A_3) \\
 m_{lht} / m_0 &= -1 / (A_2 + \frac{E_{lh0} - \lambda_\epsilon}{E_{lh0} - E_{so0}} A_4) \\
 m_{soz} / m_0 &= -1 / (A_1 + \frac{E_{so0} - \lambda_\epsilon}{E_{so0} - E_{lh0}} A_3) \\
 m_{sot} / m_0 &= -1 / (A_2 + \frac{E_{so0} - \lambda_\epsilon}{E_{so0} - E_{lh0}} A_4)
 \end{aligned} \tag{15}$$

Where A_i s correspond to the Luttinger parameters γ_i s in zinc-blend crystals. E_{lh0}, E_{so0} correspond to band edge, z direction is along the [0001] direction, and the t represents the direction transverse to z.

In Figure 6, the effective mass for heavy hole, light hole and split-off hole are presented as a function of strain.

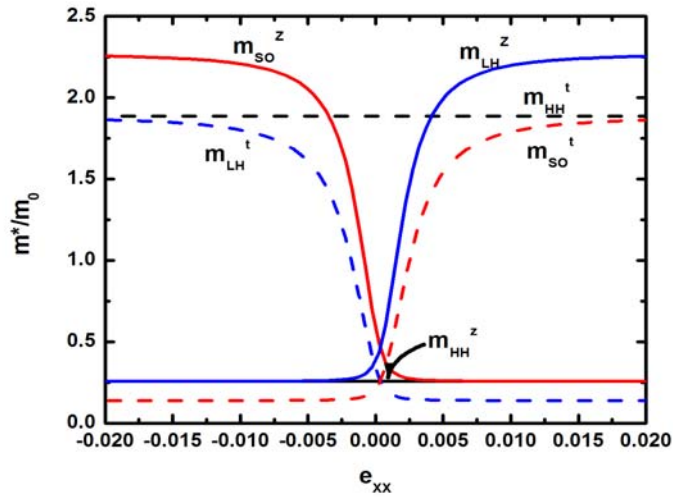


Figure 6: Schematic for effective mass as a function of strain for z and t directions

The effective mass for hole is calculated by the following equations

$$m_i = m_{hh} \frac{p_{hh}}{p_{hh} + p_{lh} + p_{so}} + m_{lh} \frac{p_{lh}}{p_{hh} + p_{lh} + p_{so}} + m_{so} \frac{p_{so}}{p_{hh} + p_{lh} + p_{so}} \quad (14)$$

Where i equals z or t, representing the mass along or transverse to z axis, p is the hole concentration.

We assume the hole carrier lifetime τ is 0.1ns [14], using the following equations, we obtain the hole mobility and conductivity as a function of strain. Figure 7,8 shows mobility and conductivity as a function of strain in both in-plane and cross-plane directions.

$$\begin{aligned} \mu_p &= q \tau / m^* \\ \sigma &= qp \mu_p \end{aligned} \quad (15)$$

Where m^* is the effective mass and p is the hole concentration.

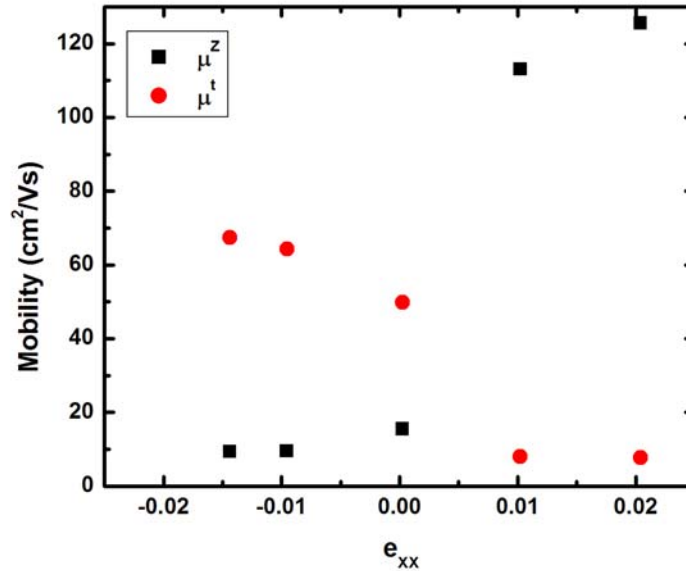


Figure 7: Mobility of holes along [0001] direction (μ^z) and transverse to [0001] direction (μ^t) as a function of strain

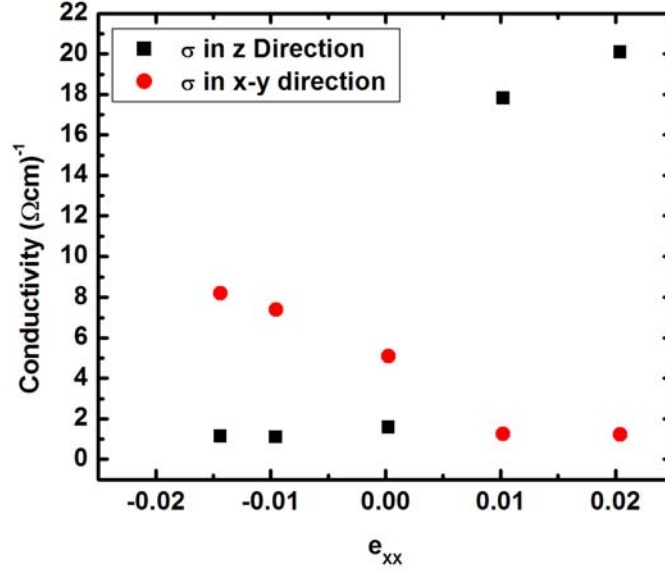


Figure 8: Conductivity along [0001] direction (σ^z) and transverse to [0001] direction (σ^t) as a function of strain

When growing real structures epitaxially one also has to worry about the critical thickness (h_c) of the material so as to avoid crystal dislocations created by the lattice mismatch. Critical thickness can be calculated numerically using [11]:

$$h_c = \frac{b \cos(\lambda)}{2\varepsilon_{xx}} \left(1 + \frac{1-\nu}{4\pi(1+\nu)\cos^2(\lambda)} \ln\left(\frac{h_c}{b}\right) \right) \quad (16)$$

Where b is the magnitude of the Burgers vector (3.189\AA in our case), λ is the angle between the Burgers vector and the misfit dislocation and ν is the Poisson ratio (assumed to be 0.3). Figure 9 shows the calculated critical thickness for GaN under different strain conditions. We can see that the critical thickness becomes very small quickly under increasing applied strain. This means that any improvement in the conductance due to an increase in the hole concentration will be limited by the thickness of the film we can grow before full relaxation of the epitaxial layer.

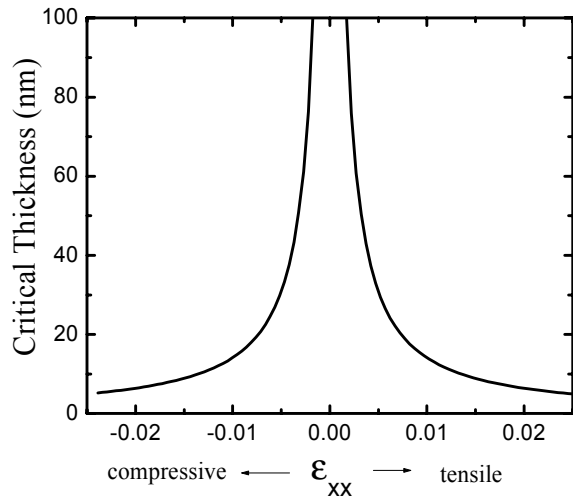


Figure 9: Critical thickness as a function of strain

We assume the sample has the area of $1\mu\text{m} \times 1\mu\text{m}$, and has been grown to the critical thickness for each strain conditions. Figure 10 shows the conductance in z direction and in x-y direction. We notice that by applying tensile strain, conductance increases in the z direction.

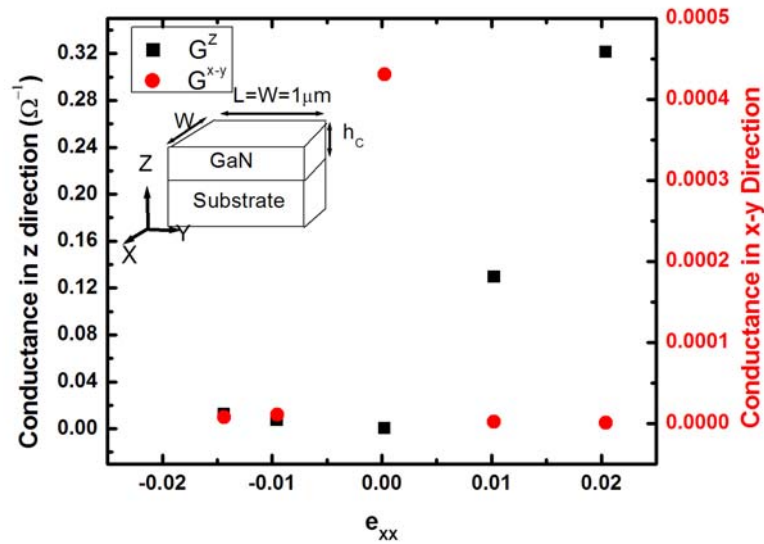


Figure 10: Conductance in z and x-y direction as a function of strain

IV. Conclusions

In this work, we have presented an analysis of the biaxial strain-modified acceptor activation energy in Mg-doped wurtzite GaN material. The change of the acceptor activation energy is caused by the strain-induced change in the band structure. Applying the k·p method on GaN developed by Prof. S.L.Chuang, we calculated the band structure of GaN under various strain.

With increasing of strain, the acceptor activation energy decreases and the hole concentration increases. The strain-induced modification is found to be more sensitive to tensile strain rather than compressive strain. Based on our analysis, the electrical properties of the p-GaN bulk material such as conductivity could be potentially improved by the induced biaxial strain, while the conductance will be limited by the critical thickness of our epitaxial layer.

Recent experimental investigations provide us with parameters different from earlier papers[6], thus our results of the band edge energies under compressive and tensile strain are more updated and may provide more accurate information for GaN related research.

Acknowledgement

The authors acknowledge Prof. Debdeep Jena for his directions and helpful discussions.

Reference

[1] H. Morkoc, S. Strite, G. B. Gao, M. E. Lin, B. Sverdlov, and M. Burns, *J. Appl. Phys.* 76, pp.1363, 1994.

[2] C. Kisielowski, J. Krüger, S. Ruvimov, T. Suski, J. W. Ager III, E. Jones, Z. Lilental_Weber, M. Rubin, E. R. Weber, M.D. Bremser, and R. R. Davis, *Phys. Rev. B* 54, pp.17745, 1996.

[3] S. L. Chuang and C. S. Chang, *Phys. Rev. B*, 54, pp.2491, 1996.

[4] Yoshitaka Nakano, Osamu Fujishima, and Tetsu Kachi, *J. Appl. Phys.* 96, pp.415 2004.

[5] K. H. Ploog and O. Brardt *J. Vac. Sci. Technol. A* 16(B), 1609 (1998).

[6] I. Vurgaftman and J. R. Meyer, “ Band parameters for nitrogen-containing semiconductors”, *J. Appl. Phys.* 94, pp.3675, 2003.

[7] S. L. Chuang and C. S. Chang, “ Effective-mass Hamiltonian for strained wurtzite GaN and analytical solutions, ” *Appl. Phys. Lett.* vol. 68, pp.1-3, 1996.

[8] M. Suzuki, T. Uenoyama, and A. Yanase, “ First-principle calculations of effective-mass parameters of AlN and GaN, ” *Phys. Rev. B*, vol. 52, pp.8132-8139, 1995.

[9] Shun Lien Chuang, “ Optical gain of strained wurtzite GaN quantum-well lasers”, *IEEE Journal of Quantum Electronics*, vol. 32, pp. 1791, 1996

[10] Peter Kozodoy, “Magnesium doped Gallium Nitride for Electronic and Optoelectronic Device Applications”, UCSB PhD Dissertation, December 1999.

[11] A. Fischer, H. Kühne and H. Richter, *Physical Review Letters* **73** (20), pp.2712, 1994

[12] K.Domen, K.Horino, A.Kuramata, and T.Tanahashi, *IEEE Journal of Selected*

Topics in Quantum Electronics, vol.3, pp.450,1997

[13] Robert F. Pierret, *Advanced Semiconductor Fundamentals*, Second Edition, Prentice Hall

[14] Michael E. Levinshtein, Sergey L. Rumyantsev, Michael S. Shur, “Properties of Advanced Semiconductor Materials”.